Journal of Hydrology 526 (2015) 196–207

Contents lists available at ScienceDirect

Journal of Hydrology

journal homepage: www.elsevier.com/locate/jhydrol

A multi-model and multi-index evaluation of drought characteristics in the 21st century

Danielle Touma [a,b,*], Moetasim Ashfaq [b], Munir A. Nayak [c], Shih-Chieh Kao [b], Noah S. Diffenbaugh [a,d]

[a] Department of Environmental Earth System Science, Stanford University, Stanford, CA, United States
[b] Climate Change Science Institute, Oak Ridge National Laboratory, Oak Ridge, TN, United States
[c] IIHR—Hydroscience and Engineering, The University of Iowa, Iowa City, IA, United States
[d] Woods Institute for the Environment, Stanford University, Stanford, CA, United States

ARTICLE INFO

Article history:
Available online 20 December 2014

Keywords:
Drought
Drought index
Climate change
CMIP5
Uncertainty
Permanent emergence

SUMMARY

Drought is a natural hazard that can have severe and long-lasting impacts on natural and human systems. Although increases in global greenhouse forcing are expected to change the characteristics and impacts of drought in the 21st century, there remains persistent uncertainty about how changes in temperature, precipitation and soil moisture will interact to shape the magnitude – and in some cases direction – of drought in different areas of the globe. Using data from 15 global climate models archived in the Coupled Model Intercomparison Project (CMIP5), we assess the likelihood of changes in the spatial extent, duration and number of occurrences of four drought indices: the Standardized Precipitation Index (SPI), the Standardized Runoff Index (SRI), the Standardized Precipitation–Evapotranspiration Index (SPEI) and the Supply–Demand Drought Index (SDDI). We compare these characteristics in two future periods (2010–2054 and 2055–2099) of the Representative Concentration Pathway 8.5 (RCP8.5). We find increases from the baseline period (1961–2005) in the spatial extent, duration and occurrence of "exceptional" drought in subtropical and tropical regions, with many regions showing an increase in both the occurrence and duration. There is strong agreement on the sign of these changes among the individual climate models, although some regions do exhibit substantial uncertainty in the magnitude of change. The changes in SPEI and SDDI characteristics are stronger than the changes in SPI and SRI due to the greater influence of temperature changes in the SPEI and SDDI indices. In particular, we see a robust permanent emergence of the spatial extent of SDDI from the baseline variability in West, East and Saharan Africa as early as 2020 and by 2080 in several other subtropical and tropical regions. The increasing likelihood of exceptional drought identified in our results suggests increasing risk of drought-related stresses for natural and human systems should greenhouse gas concentrations continue along their current trajectory.

1. Introduction

Droughts can have severe and long-lasting impacts on natural and human systems. These include humanitarian disasters, economic losses, and stresses on natural ecosystems across the globe. For example, 450,000 deaths in Ethiopia and Sudan in 1984 and 325,000 deaths in the Sahel region in 1974–1975 are directly attributed to drought (Guha-Sapir et al., 2004). Likewise, the 2012–2013 U.S. drought in the Central Plains caused more than $US12 billion in damage in the U.S. (Hoerling et al., 2013), while the 1995 drought in Spain and the 1982 drought in Australia cost $US4.5 billion and $US6 billion, respectively (Guha-Sapir et al., 2004).

In addition to mortality and economic losses, political and societal impacts can also manifest during and after drought events, especially in less economically developed nations that have limited adaptive capacity. Recurring water shortages affect 550 million people worldwide, and can cause environmental refugees to be displaced when consequent food shortages arise (Myers, 2002). For example, 20–24 million people in Sudan were affected when grain yields fell to 20% of the annual demand during a drought in 1984, and 90% of Kenyan households' food supply was in jeopardy during a 3–5 month drought period in 1999–2000 (Epule et al., 2014). Through food and water shortages, drought is also thought to have caused the displacement of one million environmental refugees in Niger is 1985 (Gemenne, 2011) and 5 million in the African Sahel in

* Corresponding author at: Stanford University, 473 Via Ortega, Suite 140, Stanford, CA 94305, United States. Tel.: +1 (919) 449 6377; fax: +1 (650) 498 5099.
E-mail address: detouma@stanford.edu (D. Touma).

http://dx.doi.org/10.1016/j.jhydrol.2014.12.011
0022-1694/

1995 (Myers, 2002). Civil conflict has also been shown to correlate with past drought events in sub-Saharan Africa (Hsiang et al., 2013), with displacement hypothesized to be either a direct or indirect contributor.

In addition to the intertwined economic, social and political effects, terrestrial ecosystems have also been subject to severe damage from drought. Anderegg et al. (2013) found that high summer temperatures and negative soil moisture anomalies were significant predictors of high aspen mortality rates associated with the unprecedented drought in Colorado in 2002. In the Amazon, mortality of large trees and lianas increased by 38% in response to an experimental four-year drought (Nepstad et al., 2007). In addition, severe drought conditions in 2005 caused a large loss in above ground biomass, causing the Amazon to store 1.2 to 1.6 petagrams less carbon that year (Phillips et al., 2009). The Mediterranean region also experienced large tree mortality rates (Allen et al., 2010) and large reductions in gross primary productivity (Ciais et al., 2005) during extreme heat wave and drought conditions in 2003.

In addition to the impacts of low soil moisture, atmospheric vapor pressure deficits, and high atmospheric temperatures on terrestrial vegetation, decreases in stream flows caused by drought can also affect aquatic ecology. For example, Poff et al. (1997) found that changes in mean monthly stream flows can affect the habitat available for aquatic organisms and the reliability of water supplies for terrestrial animals. Droughts can also cause river reaches to become isolated, causing local extirpations of species (Palmer et al., 2009). Additionally, further ecological stresses can occur when surface water deficits cause over extraction of groundwater by humans, as seen often in the Southwest U.S. (Zektser et al., 2004).

Given the widespread impacts of drought, the causes of drought in the past and the possible mechanisms by which drought could change in the future have received substantial attention in the literature. However, while the concept of drought is intuitive (i.e., a prolonged water deficit in the atmosphere, soil, and rivers), drought is caused by the complex coupling of atmospheric, hydrological and biogeophysical processes. As a result, there is no unified definition of drought (Dai, 2011). For instance, droughts do not have a clear onset, duration, or ending. In addition, the threshold for drought can vary significantly by seasons and regions, with the same amount of precipitation having different implications in wet and arid regions, or in monsoon and non-monsoon seasons. As a result, different metrics of drought highlight different variables of interest, such as precipitation for meteorologic droughts, soil moisture for agricultural droughts, and streamflow for hydrologic droughts. Mishra and Singh (2010) and Dai (2011) have presented comprehensive reviews of commonly-used drought indices, including the statistical characteristics of these indices (such as frequency, number of occurrences, and duration) that can be important for short- and long-term water management actions.

Drought assessment and preparation are further challenged by climate change. While heat extremes have intensified in recent decades and show a robust response to further global warming (e.g., IPCC (2012), Hawkins et al. (2014) and Diffenbaugh and Scherer (2011)), drought can be caused by a multitude of climate variables, and is not solely dependent on temperature or precipitation. In addition, unlike atmospheric water vapor, which is linked to atmospheric temperature through the Clausius–Clapeyron relationship, drought has no direct theoretical relationship with atmospheric temperature, and can be greatly affected by feedbacks in the climate system. Indeed, attempts to evaluate changes in drought over the instrumental record have yielded conflicting results, with contradictions attributable at least in part to discrepancies in the data used, as well as to the selection of the comparison period (Trenberth et al., 2014). The absence of a clear theoretical expectation, combined with challenges in evaluating the observed record, motivate the need to assess the mechanisms by which changes in surface temperatures and variations in precipitation patterns could influence different drought characteristics (e.g., Dai (2012), Madadgar and Moradkhani (2013), Liu et al. (2013), and Ojha et al. (2013)).

Several recent studies that used the Coupled Model Intercomparison Project Phase 3 (CMIP3) archives have shown projected drought to increase in frequency and severity in the future (e.g., Dai (2012) and Sheffield and Wood (2007)). Moreover, studies using the current CMIP5 archive have shown an increase in drought over different regions of the globe in response to continued global warming (e.g., Wang and Chen (2014) and Orlowsky and Seneviratne (2013)). However, both sets of studies have also noted the large uncertainties associated with the use of general circulation model (GCM) projections to estimate drought. Most of these uncertainties in GCM-based drought projections are a result of disagreement on the magnitude and/or sign of precipitation change, as well as the magnitude of warming (Trenberth et al., 2014). Additionally, there have been several studies that compare drought projections obtained using various drought indices, and show that the choice of methods to calculate drought characteristics can also introduce uncertainties in drought projections in the future periods (Dai, 2011; Keyantash and Dracup, 2002; Mo, 2008; Sheffield and Wood, 2007).

In addition to the publically-available global climate model archives, it is also possible to use climate variables (precipitation and temperature) as input to a hydrologic model, in order to refine the simulation of the response of the hydrologic cycle to increasing greenhouse forcing (e.g., Ashfaq et al. (2010, 2013) and van Huijgevoort et al. (2014)). However, this approach requires well-calibrated hydrologic models, as well as high-resolution climate land surface data. Given data and computational constraints, such studies have been confined to selected regions of interest where such models and data exist (e.g., the United States (Oubeidillah et al., 2014), Sweden (Andréasson et al., 2004) and Turkey (Fujihara et al., 2008)).

The sensitivity of drought assessments to physical factors such as natural variability and the interaction of multiple climate variables, and technical factors such as data availability and the definition of drought itself, motivates systematic investigation of the response of the spatial and temporal drought characteristics to increasing greenhouse gas concentrations (Wuebbles et al., 2013). Our study attempts to add to the current understanding by systematically analyzing four commonly-used drought indices using simulations from 15 GCMs available in the CMIP5 multi-model archive. We use both single- and multiple-variable indices, which allows us to separate the effects of different variables on drought. We also assess the time of emergence of statistically robust change in each drought index, which allows us to quantitatively evaluate the emergence of changes beyond the background variability. In addition, we compare the sign of change of each index across the multi-model ensemble, which allows us to quantify the level of model agreement for each index. Finally, we assess the uncertainty in the magnitude of change in each index, which allows us to understand the range of changes that are plausible over the course of the 21st century.

2. Methods

2.1. Data

We use monthly precipitation (P), temperature (T) and surface runoff (R) data from 15 Global Climate Models (GCMs) that are part of the CMIP5 data archive (Taylor et al., 2012), which were the

GCMs that had archived the necessary variables at the time of the design of our study. Following the Intergovernmental Panel on Climate Change Regional Climate Atlas (IPCC, 2013), we select the first ensemble member (r1i1p1) from each of the selected GCMs. We use bilinear interpolation, described in Wang et al. (2006), to regrid all variables from their original spatial resolution, ranging from 0.3° to 3.75° latitude and longitude (Table 1), to a common resolution of 1° horizontal grid spacing. This method is used in several multi-model studies in order to calculate uncertainty in the spatial response across an ensemble of different climate models (e.g., Burke et al. (2006), Chadwick et al. (2013), Hawkins and Sutton (2009) and Seth et al. (2013)). Given that the GCMs all have interactive land components, we rely on the output of each GCM, and do not explicitly "remodel" any of the variables in our study. For example, we depend on the land components of the individual models to take into account soil properties, topography and other relevant characteristics to simulate the surface runoff at a given grid point.

We use 45 years of the CMIP5 historical simulations, which are run until 2005, as the baseline period (1961–2005). We compare the climate of this baseline period with the Representative Concentration Pathway 8.5 (RCP8.5) simulations. In order to compare periods of equal length, we subdivide 2010–2099 into two 45-year periods (2010–2054 and 2055–2099) for the analysis. Although differences between the different pathways (RCP 2.6, 4.5, 6.0 and 8.5) are small in the next few decades, RCP8.5 is the highest emissions pathway of the four, with radiative forcing reaching 8.5 W/m^2 by the end of the 21st century, and global warming ranging from 3.9 to 6.1 °C (Rogelj et al., 2012).

2.2. Drought Indices

Although a multitude of drought indices exist (Dai, 2011), we select a subset of four indices to evaluate different types of drought: the Standardized Precipitation Index (SPI) (McKee et al., 1993), the Standard Runoff Index (SRI) (Shukla and Wood, 2008), the Standardized Precipitation–Evapotranspiration Index (SPEI) (Vicente-Serrano et al., 2010) and the Supply–Demand Drought Index (SDDI) (Table 2; Rind et al., 1990). As noted in Table 1, SRI is not calculated for CNRM-CM5 and HadGEM2-CC, since the monthly surface runoff data were not available at the time of analysis. For each GCM, the parameters that are required to calculate each drought index are derived using the 1961–2005 baseline simulation data at each grid point. The fitted parameters are then utilized to calculate the projected drought indices in the 2010–2099 period. We analyze each index at various lengths (l) of interest (e.g., 3-month) by using running averages of the variable used in that index. Though Shukla and Wood (2008), Vicente-Serrano et al. (2010) and Rind et al. (1990) use the accumulated variable to calculate SRI, SPEI and SDDI (respectively), we find that there is little to no difference between the averaged and accumulated variable in the resulting standardized drought index. (See Fig. S1, which shows the lack of difference between using the accumulated and averaged precipitation when calculating the SPI using the ACCESS1.0 model and Fig. S2, which shows differences between using the accumulated and averaged precipitation when calculating SPI the for all the 15 GCMs.) We therefore use the l-month averaged variable for all indices for consistency in our analysis.

Table 1
GCMs used for drought analysis with their original resolution in degrees latitude by degrees longitude before regridding to the common 1° resolution. Downloaded between March and June 2012.

Modeling group	GCM	Original resolution
Commonwealth Scientific and Industrial Research Organization (CSIRO) and Bureau of Meteorology (BOM), Australia	ACCESS1.0	1.25 × 1.875
Canadian Centre for Climate Modelling and Analysis (CCCMA)	CanESM2	2.77[b] × 2.8125
University of Miami—RSMAS	CCSM4	0.94[b] × 1.25
Centre National de Recherches Météorologiques/Centre Européen de Recherche et Formation Avancée en Calcul Scientifique (CNRM–CERFACS)	CNRM-CM5[a]	1.40[b] × 1.40625
Commonwealth Scientific and Industrial Research Organization in collaboration with Queensland Climate Change Centre of Excellence (CSIRO–QCCCE)	CSIRO-Mk3.6.0	1.86[b] × 1.875
NOAA Geophysical Fluid Dynamics Laboratory (GFDL)	GFDL-ESM2G	2.02[b] × 2.5
NOAA Geophysical Fluid Dynamics Laboratory (GFDL)	GFDL-ESM2M	2.02[b] × 2.5
NASA Goddard Institute for Space Studies (GISS)	GISS-E2-R	2.0 × 2.5
Met Office Hadley Centre (MOHC)	HadGEM2-CC[a]	0.34[b] × 1
Institute for Numerical Mathematics (INM)	INM-CM4	1.5[b] × 1
Institut Pierre-Simon Laplace (IPSL)	IPSL-CM5A-LR	1.89[b] × 3.75
Atmosphere and Ocean Research Institute (The University of Tokyo), National Institute for Environmental Studies, and Japan Agency for Marine-Earth Science and Technology (MIROC)	MIROC5	1.40[b] × 1.40625
Max-Planck-Institut für Meteorologie (Max Planck Institute for Meteorology) (MPIM)	MPI-ESM-LR	1.86[b] × 1.875
Meteorological Research Institute (MRI)	MRI-CGCM3	1.12[b] × 1.125
Norwegian Climate Centre (NCC)	NorESM1-M	1.89[b] × 2.5

[a] GCM not used for SRI.
[b] Resolution is approximate and varies for different latitudes.

Table 2
Drought indices used, the variables used in their calculation and the method in which the timeseries of the variables are standardized.

Drought index	Variable	Distribution(s) fitted	Standardization
SPI (McKee et al., 1993)	P	Gamma, 2-parameter lognormal	
SRI (Shukla and Wood, 2008)	R	or generalized extreme value[a]	CDF standardized to Gaussian values
SPEI (Vicente-Serrano et al., 2010)	P-PET[b]	Log–logistic	
SDDI (Rind et al., 1990)	P-PET[b]	None	Standardized using the standard deviation and the mean

[a] AIC used for distribution selection, KS and CM tests used for goodness-of-fit tests.
[b] PET calculated using the Thornthwaite method (Thornthwaite, 1948).

SPI is designed to identify precipitation deficit (for meteorologic drought), while SRI is designed to identify runoff deficit (for hydrologic drought). Although the two indices focus on different variables, their statistical concepts are similar. Based on a length (l) of interest (e.g., 3-month), these two approaches first identify a suitable probability distribution that may fit to the running averages of a variable during the baseline period. The probability distribution is then used to convert the variable into cumulative probability values and then to the standardized Gaussian values as the drought indices (Table 2). These two indices thereby provide a distribution-free, probability-based drought measure that can be compared across different locations and climates.

In this study, we fit and test three distributions, including log-normal (LN2), gamma (G2) and generalized extreme value (GEV) to identify suitable parameters for the 3-month, 6-month and 12-month SPI and SRI (Table 2). To remove seasonality, we use the sample stratification technique (Guttman, 1998). For each grid point and each GCM, we use the Akaike information criterion (AIC) to select an appropriate distribution that has the minimum AIC value. We do this to accommodate the variations in the distributions of precipitation and runoff in different geographical locations, and in different GCMs. For precipitation, the G2 distribution is found suitable in about two-thirds of the grid points across all GCMs, while for runoff both G2 and LN2 distributions fit equally well (Table 3). GEV is suitable in only 5% of the grid points for precipitation and 17% of the grid points for runoff (Table 3).

We test the goodness-of-fit for the chosen distributions in all the GCMs and indices at the 5% significance level using the Kolmogorov–Smirnov (KS) and the Cramér–von Mises (CM) tests (see Rao and Hamed (2000) and Laio (2004) for mathematical details). We found that, on average across all GCMs, 96% of the selected SPI distributions pass either the KS or CM test. However, due to the presence of extended zero values and multiple peaks often seen in GCM-simulated runoff, only 66% of the selected SRI distributions pass the KS or CM tests. The test statistics for selected SRI distributions cannot be effectively improved by using other parametric probability distributions. While the empirically-based, non-parametric approaches (e.g., kernel density estimation) could be used, we opt to use parametric distributions because the non-parametric approach is weaker for the estimation of tail distribution (i.e., for the identification of extreme droughts). Once the distribution is chosen and the parameters are calculated, the l-month averaged precipitation and runoff can be converted to the cumulative probability values and then to the standardized Gaussian values, where zero indicates the median precipitation and surface runoff, negative values indicate dry conditions, and positive values indicate wet conditions (McKee et al., 1993; Shukla and Wood, 2008).

Table 3
Percentage of grid points that use Lognormal, Gamma, and GEV distributions for fitting 6 month averaged precipitation and runoff data for the calculation of SPI and SRI respectively for each GCM. All values are in percent (%).

	Lognormal		Gamma		GEV	
	SPI	SRI	SPI	SRI	SPI	SRI
ACCESS1.0	26.5	29.2	70.0	64.6	3.5	6.1
CanESM2	29.5	49.9	67.6	16.1	2.9	34.0
CCSM4	29.7	58.8	66.8	35.2	3.5	6.0
CNRM-CM5[a]	31.0	–	66.5	–	2.5	–
CSIRO-Mk3.6.0	25.7	26.7	70.6	44.8	3.7	28.5
GFDL-ESM2G	21.6	48.7	73.3	41.7	5.2	9.6
GFDL-ESM2M	20.2	46.4	73.2	43.4	6.6	10.2
GISS-E2-R	36.1	29.3	58.7	66.2	5.3	4.5
HadGEM2-CC[a]	30.6	–	65.1	–	4.4	–
INM-CM4	26.4	48.9	68.5	39.4	5.1	11.7
IPSL-CM5A-LR	28.3	21.9	66.8	33.5	4.9	44.6
MIROC5	31.7	27.0	64.4	59.3	4.0	13.7
MPI-ESM-LR	16.3	53.4	78.6	40.2	5.1	6.4
MRI-CGCM3	31.4	45.7	66.3	13.9	2.3	40.4
NorESM1-M	27.3	53.3	68.5	40.5	4.2	6.2
Average	27.5	41.5	68.3	41.5	4.2	17.1

[a] GCM not used for SRI.

In addition to SPI (precipitation) and SRI (surface runoff), we also evaluate future drought status using SPEI and SDDI (precipitation minus potential evapotranspiration (PET), described in Section 2.2.1). Since PET represents the maximum evapotranspiration that may occur (mainly driven by temperature), the value of (P–PET) will be conceptually close to the effective precipitation value that considers the potential loss of precipitation due to temperature change. As a result, the (P–PET) based SPEI and SDDI can provide the intermediate drought measures between the processes from SPI to SRI, and can be used as surrogates to infer agricultural drought.

The stratified sampling technique is also applied to (P–PET) to remove seasonality when calculating SPEI and SDDI. To calculate SPEI, we first calculate the monthly time series of (P–PET) at each grid point with different l-month averaging periods. The log–logistic distribution (LL2) is then fitted to (P–PET) and standardized in the same way as SPI and SRI (Vicente-Serrano et al., 2010) (Table 2). To calculate the SDDI, we use the standard deviations and means of the anomalies of (P–PET) in the baseline period to standardize the time series of (P–PET) of l-month averaging periods over the baseline and future periods (Table 2; Rind et al., 1990).

$$Z_{i,j,m} = \frac{(P - PET)_{i,j,m} - \mu_{j,m}}{\sigma_{j,m}} \quad (1)$$

In Eq. (1), $Z_{i,j,m}$ is the standardized (P–PET) at year i, grid point j and month m, $\mu_{j,m}$ and $\sigma_{j,m}$ are the mean value and standard deviation of (P–PET) at month m and grid point j, respectively. Once a time series of Z is achieved, the current SDDI is calculated by adding a fraction of the previous month's SDDI value to the Z current value (Rind et al., 1990).

$$\mathrm{SDDI}_{n,j} = 0.897 * \mathrm{SDDI}_{n-1,j} + Z_{n,j} \quad (2)$$

In Eq. (2), $\mathrm{SDDI}_{n,J}$ is the SDDI value at time step n and grid point j, and $\mathrm{SDDI}_{0,J} = Z_{0,j}$. Similar to the other indices, negative values of SDDI indicate dry conditions and positive values indicate wet conditions.

2.2.1. Potential evapotranspiration

We estimate the monthly potential evapotranspiration (PET) at each grid point using the Thornthwaite equations (Thornthwaite, 1948), where

$$PET = 16\left(\frac{L}{12}\right)\left(\frac{N}{30}\right)\left(\frac{10T}{I}\right)^{a}, \quad (3)$$

$$i = \left(\frac{T}{5}\right)^{1.514} \quad (4)$$

$$a = (6.75 \times 10^{-7})I^3 - (7.71 \times 10^{-5})I^2 + (1.792 \times 10^{-2})I + 0.49239 \quad (5)$$

In Eqs. (3)–(5), PET is in mm/month, T is the average daily temperature of the month in degrees Celsius, N is the number of days in that month, L is the average day length of that month in hours, I is a heat index equaling to the sum of 12 monthly index values of i (Eq. (4)), and a is an empirically derived exponent that is a function of I.

Although there are other alternative methods to estimate PET, such as the Penman and Penman–Monteith equations, we select the Thornthwaite method because it relies solely on the average temperature and length of day of each month. Although the Thornthwaite method may be over simplified compared with other

approaches, it has been shown that the choice of methods in the calculation of *PET* does not critically influence the outcome of drought projections (Burke et al., 2006).

2.3. Definition of drought

We analyze five levels of drought severity based on US Drought Monitor classifications (Svoboda et al., 2002): D0 (abnormally dry, 20–30% percentile), D1 (moderate drought, 10–20%), D2 (severe drought, 5–10%), D3 (extreme drought, 2–5%) and D4 (exceptional drought, <2%). For each grid point in each GCM, we find the thresholds corresponding to each level of drought based on the percentile of the 1961–2005 baseline period. For example, to find the D4 drought threshold for the SPI for a grid point (e.g., 39.5 N, 120.5 W) over Western North America in the ACCESS1.0 GCM, we find the 2nd percentile of the SPI time series in the ACCESS1.0 baseline simulation (e.g., −2.1). This value is then considered to be the D4 threshold for that grid point in the ACCESS1.0 GCM. Any month in either the baseline period or future sub-periods that the SPI for that grid point falls below this threshold (i.e., SPI < −2.1) is considered to be a D4 drought month. Similarly, we apply this method for all drought levels in each drought index and each GCM.

Although we assess the characteristics of the 3-month, 6-month and 12-month drought for all indices and all levels of drought (D0–D4), we focus our results and discussion on the characteristics of the 6-month "exceptional" (D4) drought, including differences among the various climate models and drought indices.

2.4. Drought characteristics

We investigate the characteristics of drought in each index and at each level of drought severity. For a given level of drought severity, we define (1) a *drought event* as a continuous period of time when the drought index in each month is below that level, (2) the *duration* of drought as the length of a drought event in months, (3) the *occurrence* of drought as the total number of drought events in the entire study period (i.e., baseline or future), and (4) the *spatial extent* of drought as the percentage of grid points in which the drought index falls below the given drought level each month. We quantify the drought characteristics over the regions defined by Giorgi and Bi (2005). In order to account for differences in actual grid sizes, we calculate the area-weighted regional mean using the cosine of latitude.

We calculate the difference in drought characteristics between the baseline and 21st century periods. In addition, to understand the robustness of the change in the spatial extent of drought in the future, we find the *decade of emergence* in which the change permanently exceeds the baseline variability. More specifically, we calculate the year at which the changes in spatial extent for each region permanently exceeds two standard deviations of the anomalies of the spatial extent of that region during the baseline period (e.g., Diffenbaugh et al. (2011)). We calculate this time of emergence for each GCM for each region, and define the *decade of emergence* for that region as the decade in which the median time of emergence of the GCMs occurs, although the time of emergence for certain models may fall outside the decade of emergence.

3. Results and discussion

3.1. Changes in 21st century precipitation and temperature

Since the drought indices that we use are highly dependent on temperature and precipitation, we first evaluate the response of mean precipitation and temperature in the 21st century of RCP8.5. Fig. 1 shows simulations from the 15 GCMs we use in this study (Table 1). These simulations show a mean increase in temperature of 1.8 °C for 2010–2054 and 4.2 °C for 2055–2099. Higher temperatures (usually associated with greater rates of evapotranspiration) are expected to lead to higher levels of frequency of drought. However, there is also an increase in mean precipitation over land (2% in 2010–2054 and 6% in 2055–2099), which could reduce some of the impact of increasing temperature. Given the interwoven and nonlinear relationships among precipitation, temperature and other hydro-meteorological variables in different regions, it is imperative to examine the overall drought status using multiple indices that span different phases of the hydrologic cycle.

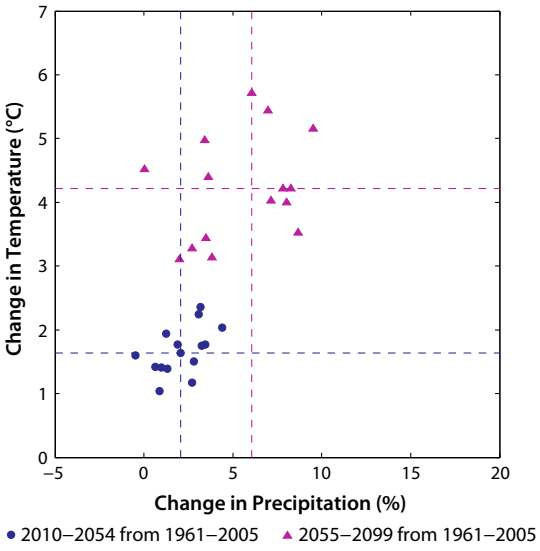

Fig. 1. Change of mean global land surface precipitation (%) versus temperature (°C) for early future (2010–2054) and late future (2055–2099) from the baseline period (1961–2005) for each GCM. The dashed lines mark the GCM ensemble median.

3.2. Changes in 21st century drought characteristics

3.2.1. Spatial extent of drought

Fig. 2 shows the 21st century time series of projected change of D4 6-month spatial extent for all indices in the 26 regions. Since the severity levels are derived using the baseline model simulations, the D4 spatial extent in the baseline period is approximately 2%. In all regions, the SPEI and SDDI show the largest changes in spatial extent, especially in the tropical and subtropical regions during the 21st century period. For instance, South Asia (SAS) and Central Asia (CAS) exhibit an increase of approximately 50% in the SPEI spatial extent and 80% in the SDDI spatial extent by the end of 21st century, but show little changes in SPI and SRI spatial extent. On the other hand, extra-tropical regions such as Western North America (WNA) and Central North America (CNA) show more moderate increase in the SPEI and SDDI (<30% and <60% respectively) spatial extent, and some increase (>10%) in the SRI frequency by the end of 21st century. However, nearly all regions show no noticeable changes in the SPI spatial extent of drought, with the exception of the Mediterranean (MED), Southern South America (SSA), and Central America (CAM), where increases of <10% are exhibited by the end of 21st century.

To test the statistical robustness of the simulated changes of spatial extent, we also calculate the decade of emergence. Given that the model simulations are restricted to the 21st century, we follow Diffenbaugh et al. (2011) and Diffenbaugh and Scherer (2011) in only considering emergence prior to 2080 to be permanent. The SDDI spatial extent of drought shows a median decade

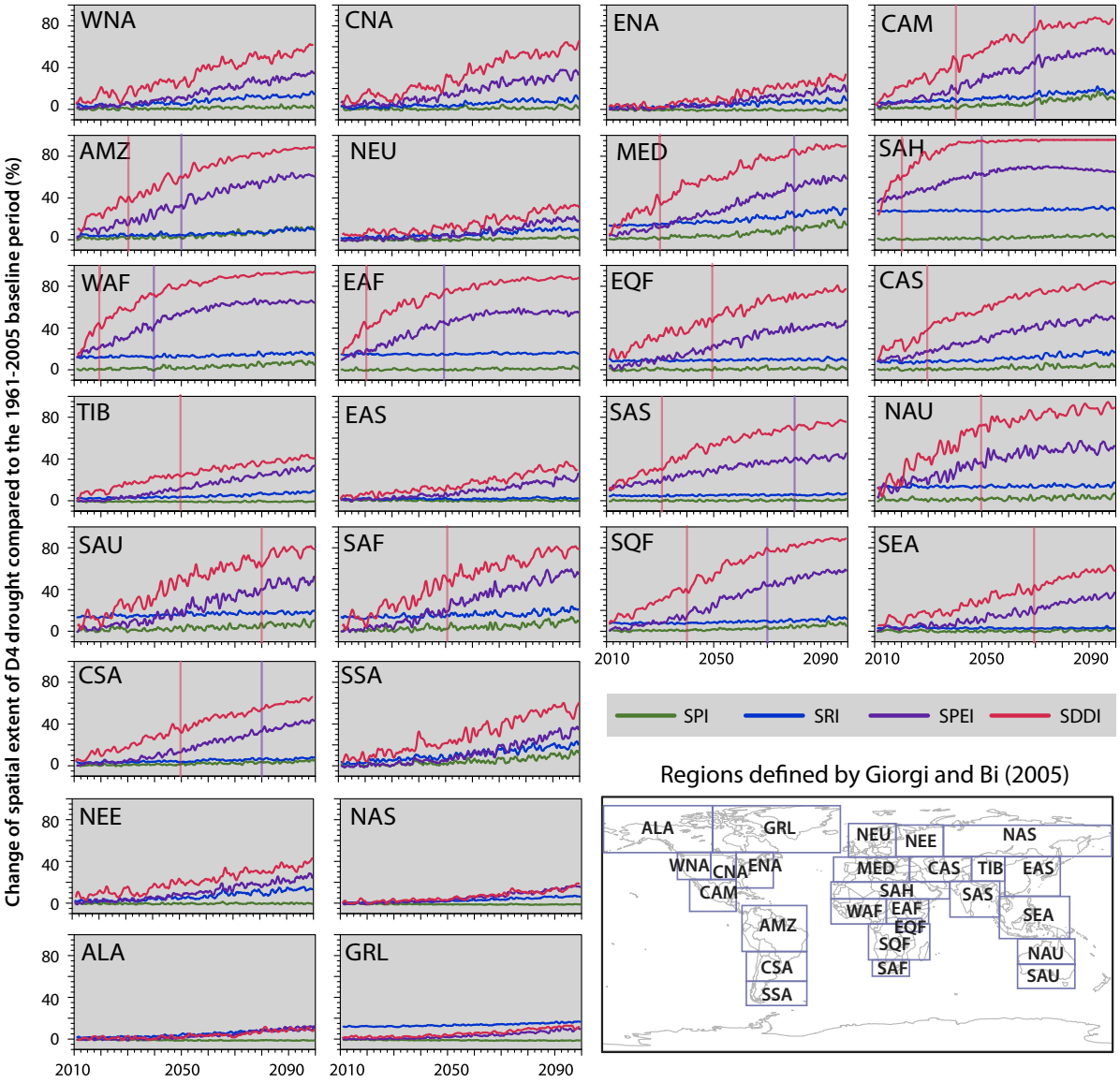

Fig. 2. Change of spatial extent of SPI, SRI, SPEI and SDDI 6-month D4 drought in the future period (2010–2099) relative to the baseline period (1961–2005). The time series shows the change of annual GCM ensemble mean spatial extent for each region defined by Giorgi and Bi (2005). The vertical lines mark the median decade of emergence for each region and for each index. Missing vertical lines indicate no permanent emergence of the spatial extent of drought by 2080 for the corresponding region and index.

of emergence prior to 2080 for 15 subtropical and tropical regions, with the Sahara (SAH), East Africa (EAF) and West Africa (WAF) showing median emergence in the 2020s (Fig. 2). The SPEI spatial extent of drought shows a median decade of emergence for nine regions, with the earliest decade of emergence occurring in the 2040s in WAF. On the other hand, there are no regions with changes in spatial extent that permanently exceed two standard deviations of the baseline variability of SPI and SRI during the 21st century of RCP8.5.

3.2.2. Occurrence of drought events

Fig. 3 shows the spatial pattern of changes in the occurrences of 6-month D4 drought episodes in the early (2010–2054) and late (2055–2099) 21st century periods. Additionally, we have quantified the agreement among the GCMs in the projections to address the uncertainty in the multi-model projections. In general, the SPI shows the least agreement and the SPEI shows the most agreement among the GCMs. The SPI shows greater agreement among the models over CAM, Amazon (AMZ), South Africa (SAF) and MED, all of which exhibit greater occurrences of the D4 drought episodes in the late 21st century period. Similarly, the SRI and SPEI show larger changes and greater agreement among models in the late 21st century period (Fig. 3b, d and f). In contrast, the SDDI shows changes occurring in different regions for each of the two future periods (Fig. 3g and h). For example, AMZ shows increases of approximately 10 SDDI drought occurrences in the 45 years of the early 21st century period, but no changes in the later period. Comparatively, CAS shows increases of approximately 10 SDDI drought occurrences in the 45 years of the early 21st century period, but decreases of approximately 3 occurrences in the later period (Fig. 3g and h). It is important to note that these decreases in occurrence do not necessarily imply fewer total months of drought, as the drought events could be longer in duration and therefore show fewer separate occurrences during the 45-year period (see Section 3.2.3 below).

Our analysis shows that even if a region exhibits strong agreement in the sign of change among the GCMs, there could still be a discrepancy in the magnitude of this change, unveiling

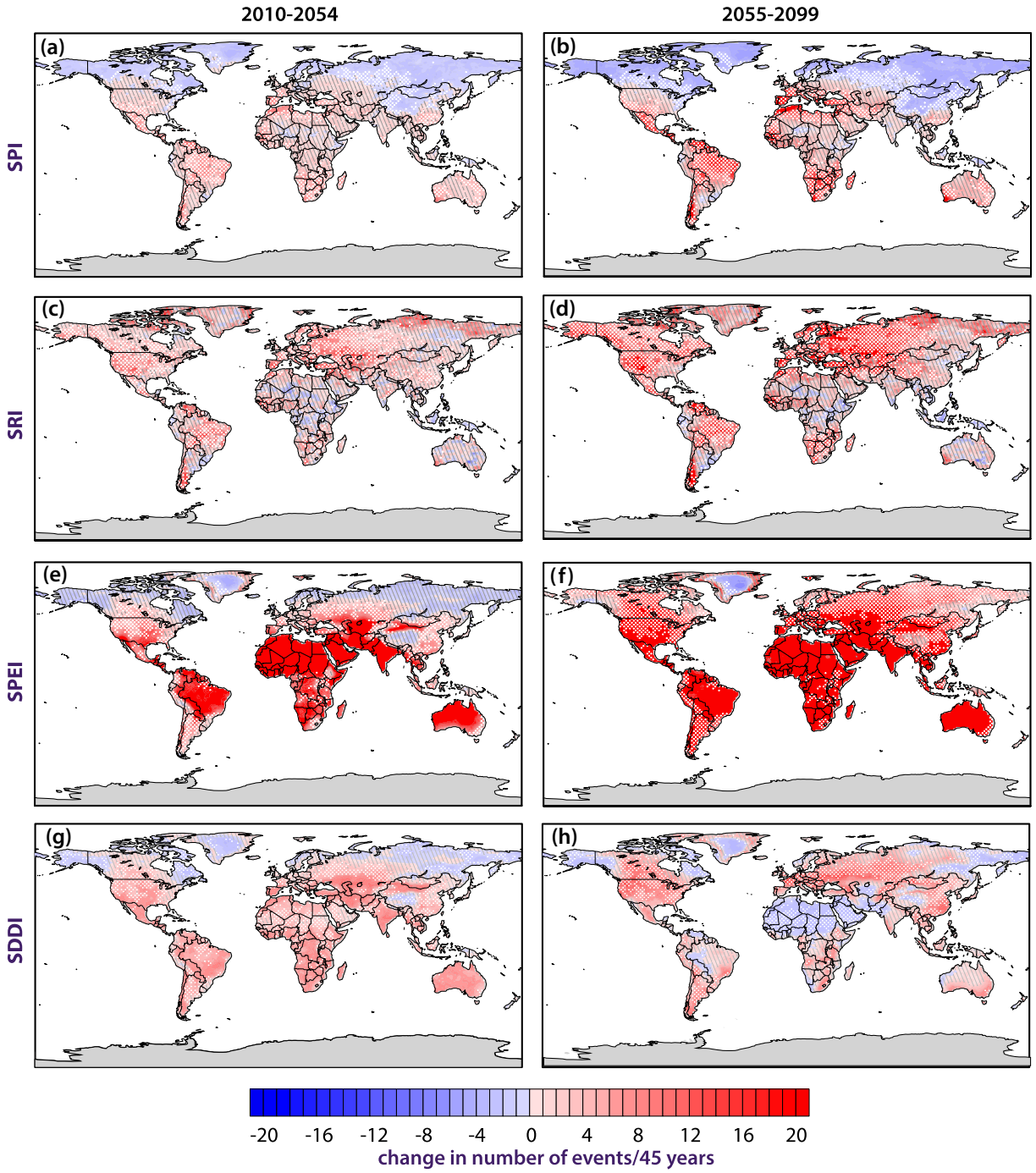

Fig. 3. Change of 6-month D4 drought occurrence in the early future period (2010–2054) and late future period (2055–2099) relative to the baseline period (1961–2005), using (a, b) SPI, (c, d) SRI, (e, f) SPEI and (g, h) SDDI. The color shows the GCM ensemble mean. Areas with no stippling indicate where 90% or more of the GCMs agree on the sign of change, the white stippling shows where at least two-thirds of the GCMs agree on the sign of change and the grey lines show where less than two-thirds of the GCMs agree on the sign of change.

the uncertainty among the GCMs. For example, the SPEI and SDDI show strong agreement (among at least two-thirds of GCMs) in the sign of change of D4 6-month drought occurrences over Western and Central North America in the late 21st century period (Fig. 3f and h). However, the spread in the magnitude of the changes is large (Fig. 4g and h). The CNA region shows a change in SDDI occurrence ranging from an increase of 3 to 13 events in 45 years and a change in SPEI occurrence ranging from a decrease of 10 events to an increase of 40 events in 45 years. On the other hand, other regions, including Central South America (CSA) and SSA, show strong agreement in the sign of change in SPEI and SDDI occurrence in the late 21st century period (Fig. 3f and h), and also exhibit a relatively small spread in the magnitude of change (Fig. 4g and h). Although there are differences in the inter-model spread for the change in occurrences between the two 21st century periods, the spread tends to be greater over most regions for the later period.

3.2.3. Duration of drought events

Fig. 5 shows the spatial pattern of changes in the duration of D4 drought episodes in the 2010–2054 and 2055–2099 periods of RCP8.5. The mean duration of 6-month D4 drought events is still

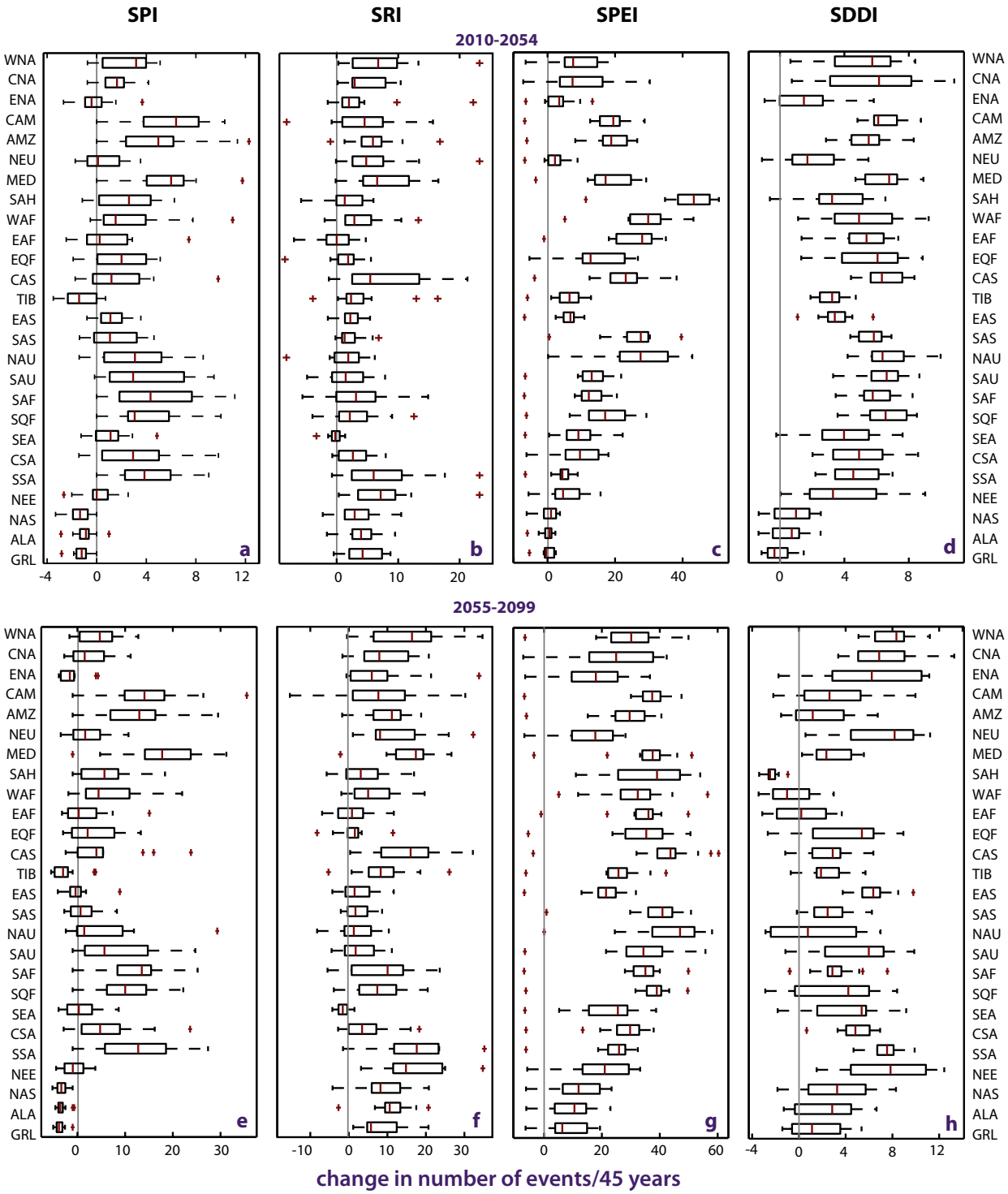

Fig. 4. Change of 6-month D4 drought occurrence in 2010–2054 (a–d) and 2055–2099 (e–h) relative to the baseline period (1961–2005) for each region using (a, e) SPI, (b, f) SRI, (c, g) SPEI and (d, h) SDDI. The range of the GCM ensemble is shown, where the center line in the box is the 50th percentile of the ensemble, the left and right boundaries of the box represent the 25th and 75th percentiles respectively and the red crosses show the outliers which fall approximately outside the 99th percentile in the GCM datasets. The region definitions are from Giorgi and Bi (2005) as seen in Fig. 2.

relatively low in the 2010–2054 period (Fig. 5a, c, e and g), with the exception of SDDI, which shows long-lasting drought events in SAH and AMZ (Fig. 5g). The 2055–2099 period shows much longer SPEI and SDDI drought durations (Fig. 5f and h), where SAH and AMZ have SDDI and SPEI drought events longer than 10 and 3 years, respectively. These large increases in the duration of SDDI episodes help to explain the decreases in drought occurrence over these regions (Section 3.2.2), as large increases in duration tend to reduce number of individual occurrences, particularly for very long duration events. In contrast, the higher latitudes tend to show relatively little change in drought duration, even in the 2055–2099 period. Changes in drought characteristics in these higher latitude

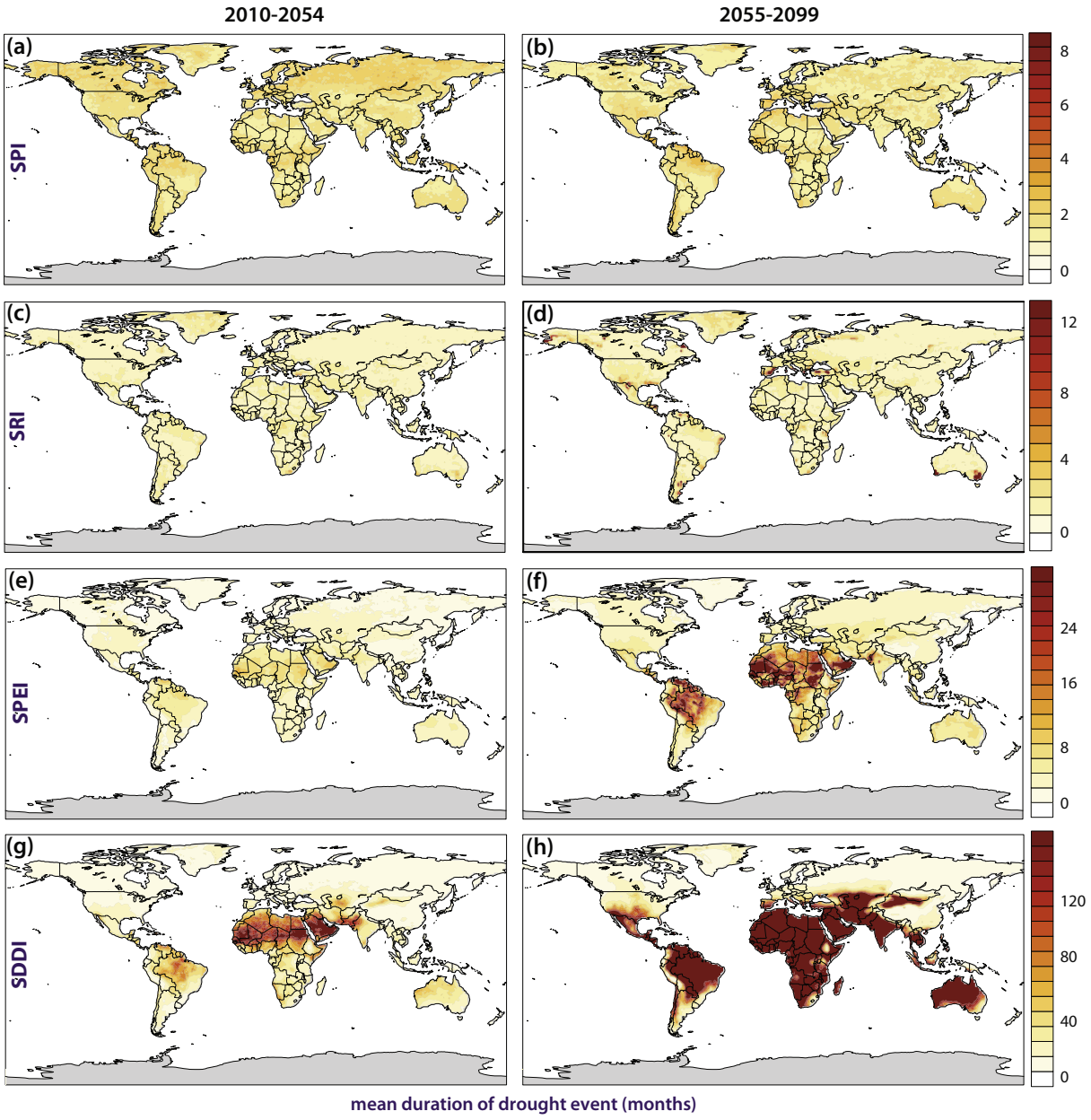

Fig. 5. GCM ensemble mean duration of a 6-month D4 drought event in 2010–2054 (a–g) and 2055–2099 (b–h) for the SPI (a, b), SRI (c, d), SPEI (e, f) and SDDI (g, h). In the baseline period (1961–2005), the mean duration is between 1 and 2 months for all regions and all indices (not shown here).

regions can therefore be explained predominantly by changes in drought occurrence.

Fig. 6 captures the relationship between the ensemble-median changes in drought duration and occurrence for the 26 regions. In most of the regions, there is an increase in both the occurrence and duration of drought. Exceptions include the SAH and WAF regions in the 2055–2099 period, where the SDDI duration of drought increases by more than 500 and 420 months respectively, but the occurrence of drought decreases (Fig. 6h). These large increases in the SDDI duration of drought can also be inferred from the spatial extent of drought in SAH and WAF (Fig. 2). In these regions, the SDDI spatial extent increases and remains high, with >80% of the regions being under D4 drought throughout the 2055–2099 period. The large extent of D4 drought can be explained by the large increases in global temperature (Fig. 1) in the 2055–2099 period in RCP8.5, (which range spatially from 2 °C to 11 °C (IPCC, 2013)). which in turn explain the decreases in the deficit (*P–PET*). In addition, the non-parametric standardization of the deficit used in the calculation of the SDDI allows the SDDI to decrease continuously and rapidly throughout the 21st century, resulting in large increases in the duration of SDDI drought.

In contrast, several areas, including Eastern North America (ENA), Greenland (GRL), Alaska (ALA) and North Asia (NAS) regions show decreases, albeit small, in both the occurrences and duration of SPI drought events in the 2050–2099 period (Fig. 6b). In the same period, there is also a minimal decrease in occurrences and duration of SRI events in Southeast Asia (SEA) (Fig. 6d). Moreover, in 2010–2054, the changes in the occurrence of SPEI and SDDI are large, while the changes in duration are small for most regions (Fig. 6e and g). On the other hand, the 2055–2099 period shows large increases in both the occurrence and duration of SPEI and SDDI (Fig. 6f and h). The 2010–2054 period shows similar changes in SPI and SRI duration and occurrence among the regions, while the 2055–2099 period shows regions where the SPI and SRI

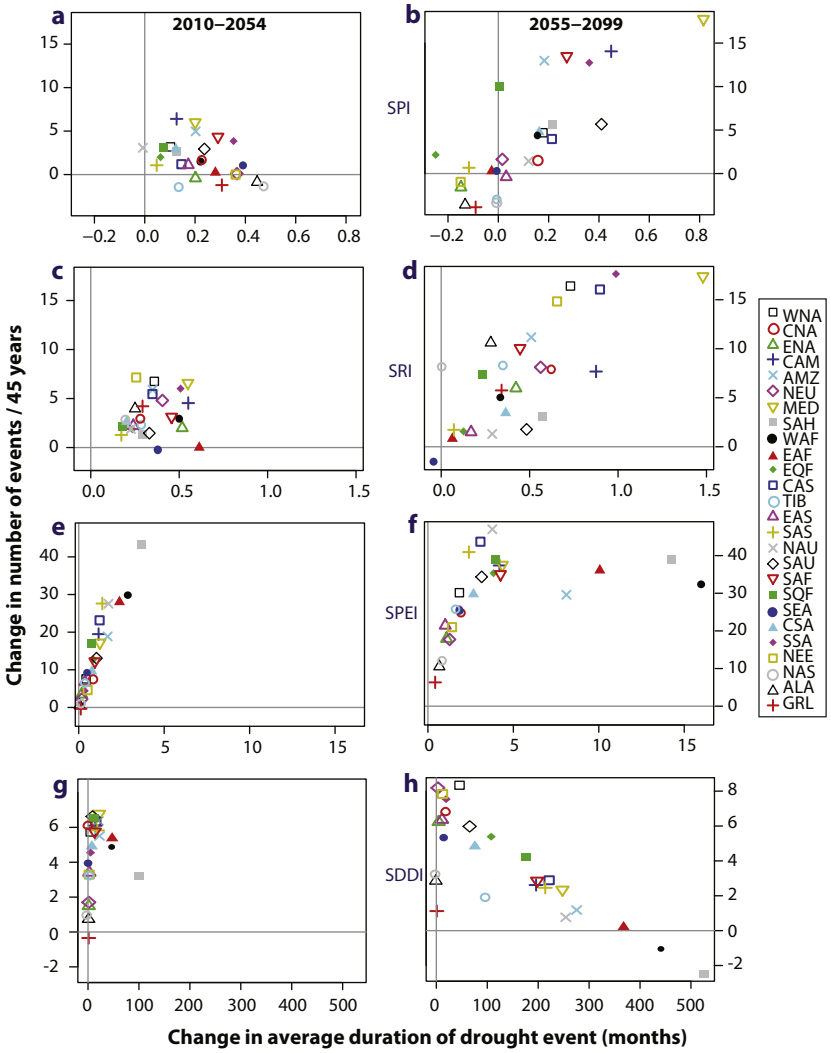

Fig. 6. GCM ensemble median change in the number of drought events related to the GCM ensemble median change in the average duration of a drought event from the baseline period (1960–2005) for 2010–2054 (a, c, e, g) and 2055–2099 (b, d, f, h) for SPI (a, b), SRI (c, d), SPEI (e, f) and SDDI (g, h) for each region. The region definitions are from Giorgi and Bi (2005) as seen in Fig. 2.

duration and occurrence are more responsive to the RCP 8.5 forcing (Fig. 6a–d), with the MED, AMZ, CAM and SSA being examples of this stronger response.

3.3. Multi-index and multi-model assessments

Our analysis shows that many regions exhibit increases in the spatial extent, duration and occurrence of drought in the 21st century of the RCP8.5 pathway. However, by using multiple GCMs and multiple indices we also highlight the uncertainty of the responses of the drought characteristics.

The smallest increases occur in the SPI spatial extent and duration of drought (Figs. 2 and 5), even in locations where all other indices show relatively large increases. However, there are some noticeable increases in occurrence (Fig. 3). Areas where SPI occurrence increases tend to correspond to decreases in the annual precipitation in RCP8.5 (Diffenbaugh and Field, 2013), suggesting that decreases in annual precipitation over the 21st century could lead to greater SPI drought occurrence, but not necessarily greater spatial extent or duration.

Alternatively, stronger increases in the spatial extent, duration and occurrence are seen in SPEI and SDDI, along with greater agreement on the sign of change among the GCMs. Although these indices take both precipitation and temperature into account, it is clear that they are highly responsive to the temperature changes that occur in RCP8.5 (Fig. 1), with the largest increases in SPEI and SDDI drought occurrence, duration and spatial extent co-occurring with the largest increases in annual temperature (i.e., over North and West Africa and the Mediterranean and Amazon regions) (Diffenbaugh and Field, 2013). The effect of these changes in temperature is therefore amplified in the SDDI and SPEI, which use temperature as the sole, non-stationary variable, as defined in the Thornthwaite equation for PET. However, we note that when Cook et al. (2014) use the Penman–Monteith method for PET, they also find that PET is the main contributor to large decreases in the average SPEI index in 2080–2099 in RCP8.5 over most of the globe. Therefore, irrespective of PET method choice, large increases in drought are projected in the 21st century when using a deficit variable (*P–PET*).

We note a number of important caveats to our analyses. The changes in SRI drought characteristics in this study reflect the changes in surface runoff and not the total runoff, as originally studied by Shukla and Wood (2008). We can better represent drought characteristics by using the total runoff, which responds to changes in climate variables at longer time scales, rather than using surface runoff, which responds to changes at shorter, more

instantaneous timescales. Therefore, the absence of sub-surface runoff in our analysis could potentially enhance the spread among the GCMs' simulated responses and cause low agreement among the GCMs as seen in Figs. 3 and 4.

We also note that our study does not include a soil moisture index, which could alter the range of responses of the drought characteristics. Orlowsky and Seneviratne (2013) use the soil moisture anomaly to quantify drought in the CMIP5 ensemble. Similar to our study, they find large increases in drought frequency in many regions, although the soil-moisture-based changes are smaller in magnitude than the changes we identify using the SPEI and SDDI.

In addition, because our drought severity categories (D0–D4) are defined relative to the baseline variability, biases in the simulated variability could influence the results. For example, insufficient variability in the baseline period could enhance the simulated increase in drought occurrence resulting from a given simulated temperature trend, and show an earlier decade of emergence.

Finally, it is important to emphasize that even in regions where there is strong agreement on the sign of the change in occurrences of drought events (Fig. 3), there are still large discrepancies in the magnitude of these changes among the GCMs. This result expands on previous drought studies that also find large uncertainties among GCMs when projecting drought into the 21st century using either the CMIP3 or the CMIP5 ensemble (Dai, 2012; Orlowsky and Seneviratne, 2013; Sheffield and Wood, 2007). In addition, uncertainty arising from internal variability and emissions pathway (Hawkins and Sutton, 2009) could potentially create further uncertainty in the drought indices. In fact, Orlowsky and Seneviratne (2013) find that although internal variability can be the main source of uncertainty in SPI drought projections, the spread among the GCMs can overwhelm both scenario uncertainty and internal variability in shaping uncertainty in soil moisture anomaly projections for the late 21st century. However, although the GCM uncertainties, in our study and others, can be large and variable among indices and regions, we extend the analysis by showing the strength of agreement (or disagreement) of the GCMs on the sign of change in the occurrence of drought in the 21st century (Fig. 3).

4. Conclusions

We find that spatial extent, occurrence and duration of "exceptional" (D4) drought increase in subtropical and tropical regions in all four drought indices in the 21st century of the RCP8.5 pathway. Additionally, the increases in SPEI and SDDI drought extend into the higher latitudes, including Southern South America, South Africa and Southern Australia in the southern hemisphere, and Northeastern Europe and Central North America in the northern hemisphere. In addition, we find high agreement in the sign of the change over many areas of the globe, including emergence of changes in the frequency of drought that permanently exceed two standard deviations of the baseline variability in multiple regions.

Our results have important implications for near- and long-term climate risk management. Given that the risk of impacts on human and natural systems results from the intersection of hazard, exposure and vulnerability (Oppenheimer et al., 2014), increases in the likelihood of drought hazards implies increasing risk for drought-sensitive systems. For regions to manage these drought risks, both local and inter-regional water management policies will likely have to be modified and adapted in the coming decades, as existing water management practices are unlikely to be able to reduce negative impacts of drought on water supply reliability and aquatic systems (Kundzewicz et al., 2008). In addition, global mitigation of greenhouse gas emissions could prevent or postpone the permanent emergence of increasing drought frequency, thereby reducing the risks for humans and ecosystems.

Acknowledgements

We thank the editor, guest editor and three anonymous reviewers for their insightful and constructive comments. Support for data storage and analysis is provided by the Oak Ridge Leadership Computing Facility at the Oak Ridge National Laboratory, which is supported by the Office of Science of the U.S. Department of Energy under Contract No. DE-AC05-00OR22725. We acknowledge the World Climate Research Program's Working Group on Coupled Modeling responsible for CMIP, and we thank the climate modeling groups for producing and making available their CMIP5 model output. We also thank U.S. Department of Energy's Program for Climate Model Diagnosis and Intercomparison for providing coordinating support and leading development of software infrastructure in partnership with the Global Organization for Earth System Science Portals for CMIP. This work at Oak Ridge National Laboratory is supported by Regional and Global Climate Modeling program of DOE Office of Science and Oak Ridge National Laboratory LDRD project 32112413, and the work at Stanford was supported in part by NSF award #0955283 to NSD.

Appendix A. Supplementary material

Supplementary data associated with this article can be found, in the online version, at http://dx.doi.org/10.1016/j.jhydrol.2014.12.011.

References

Allen, C.D., Macalady, A.K., Chenchouni, H., Bachelet, D., McDowell, N., Vennetier, M., Kitzberger, T., Rigling, A., Breshears, D.D., Hogg, E.H., Gonzalez, P., Fensham, R., Zhang, Z., Castro, J., Demidova, N., Lim, J.-H., Allard, G., Running, S.W., Semerci, A., Cobb, N., 2010. A global overview of drought and heat-induced tree mortality reveals emerging climate change risks for forests. For. Ecol. Manage. 259, 660–684. http://dx.doi.org/10.1016/j.foreco.2009.09.001.

Anderegg, L.D.L., Anderegg, W.R.L., Abatzoglou, J., Hausladen, A.M., Berry, J.A., 2013. Drought characteristics' role in widespread aspen forest mortality across Colorado, USA. Glob. Chang. Biol. 19, 1526–1537. http://dx.doi.org/10.1111/gcb.12146.

Andréasson, J., Bergström, S., Carlsson, B., Graham, L.P., Lindström, G., 2004. Hydrological change – climate change impact simulations for Sweden. Ambio 33, 228–234.

Ashfaq, M., Bowling, L.C., Cherkauer, K., Pal, J.S., Diffenbaugh, N.S., 2010. Influence of climate model biases and daily-scale temperature and precipitation events on hydrological impacts assessment: A case study of the United States. J. Geophys. Res. 115, D14116. http://dx.doi.org/10.1029/2009JD012965.

Ashfaq, M., Ghosh, S., Kao, S.-C., Bowling, L.C., Mote, P., Touma, D., Rauscher, S.A., Diffenbaugh, N.S., 2013. Near-term acceleration of hydroclimatic change in the western U.S. J. Geophys. Res. Atmos. 118 (10), 676–10,693. http://dx.doi.org/10.1002/jgrd.50816.

Burke, E.J., Brown, S.J., Christidis, N., 2006. Modeling the recent evolution of global drought and projections for the twenty-first century with the Hadley Centre climate model. J. Hydrometeorol. 7, 1113–1126.

Chadwick, R., Boutle, I., Martin, G., 2013. Spatial patterns of precipitation change in CMIP5: Why the rich do not get richer in the tropics. J. Clim. 26, 3803–3822. http://dx.doi.org/10.1175/JCLI-D-12-00543.1.

Ciais, P., Reichstein, M., Viovy, N., Granier, A., Ogée, J., Allard, V., Aubinet, M., Buchmann, N., Bernhofer, C., Carrara, A., Chevallier, F., De Noblet, N., Friend, A.D., Friedlingstein, P., Grünwald, T., Heinesch, B., Keronen, P., Knohl, A., Krinner, G., Loustau, D., Manca, G., Matteucci, G., Miglietta, F., Ourcival, J.M., Papale, D., Pilegaard, K., Rambal, S., Seufert, G., Soussana, J.F., Sanz, M.J., Schulze, E.D., Vesala, T., Valentini, R., 2005. Europe-wide reduction in primary productivity caused by the heat and drought in 2003. Nature 437, 529–533. http://dx.doi.org/10.1038/nature03972.

Cook, B.I., Smerdon, J.E., Seager, R., Coats, S., 2014. Global warming and 21st century drying. Clim. Dyn. http://dx.doi.org/10.1007/s00382-014-2075-y.

Dai, A., 2011. Drought under global warming: a review. Wiley Interdiscip. Rev. Clim. Chang. 2, 45–65. http://dx.doi.org/10.1002/wcc.81.

Dai, A., 2012. Increasing drought under global warming in observations and models. Nat. Clim. Chang. 3, 52–58. http://dx.doi.org/10.1038/nclimate1633.

Diffenbaugh, N.S., Ashfaq, M., Scherer, M., 2011. Transient regional climate change: analysis of the summer climate response in a high-resolution, century-scale, ensemble experiment over the continental United States. J. Geophys. Res. 116, 1–16. http://dx.doi.org/10.1029/2011JD016458.

Diffenbaugh, N.S., Field, C.B., 2013. Changes in ecologically critical terrestrial climate conditions. Science 341, 486–492. http://dx.doi.org/10.1126/science.1237123.

Diffenbaugh, N.S., Scherer, M., 2011. Observational and model evidence of global emergence of permanent, unprecedented heat in the 20th and 21st centuries. Clim. Change 107, 615–624. http://dx.doi.org/10.1007/s10584-011-0112-y.

Epule, T.E., Peng, C., Lepage, L., 2014. Environmental refugees in sub-Saharan Africa: a review of perspectives on the trends, causes, challenges and way forward. GeoJournal 343, 1–14. http://dx.doi.org/10.1007/s10708-014-9528-z.

Fujihara, Y., Tanaka, K., Watanabe, T., Nagano, T., Kojiri, T., 2008. Assessing the impacts of climate change on the water resources of the Seyhan River Basin in Turkey: Use of dynamically downscaled data for hydrologic simulations. J. Hydrol. 353, 33–48. http://dx.doi.org/10.1016/j.jhydrol.2008.01.024.

Gemenne, F., 2011. Climate-induced population displacements in a 4 °C+ world. Philos. Trans. A. Math. Phys. Eng. Sci. 369, 182–195. http://dx.doi.org/10.1098/rsta.2010.0287.

Giorgi, F., Bi, X., 2005. Updated regional precipitation and temperature changes for the 21st century from ensembles of recent AOGCM simulations. Geophys. Res. Lett. 32, L21715. http://dx.doi.org/10.1029/2005GL024288.

Guha-Sapir, D., Hargitt, D., Hoyois, P., 2004. Thirty Years of Natural Disasters 1974-2003: The Numbers. Presses universitaires de Louvain, Louvain-la-Neuve, Belgium.

Guttman, N., 1998. Comparing the palmer drought index and the standardized precipitation index. J. Am. Water Resour. Assoc. 34.

Hawkins, E., Anderson, B., Diffenbaugh, N., Mahlstein, I., Betts, R., Hegerl, G., Joshi, M., Knutti, R., McNeall, D., Solomon, S., Sutton, R., Syktus, J., Vecchi, G., 2014. Uncertainties in the timing of unprecedented climates. Nature 511. http://dx.doi.org/10.1038/nature13523, E3–5.

Hawkins, E., Sutton, R., 2009. The potential to narrow uncertainty in regional climate predictions. Bull. Am. Meteorol. Soc. 90, 1095–1107. http://dx.doi.org/10.1175/2009BAMS2607.1.

Hoerling, M., Schubert, S., Mo, K.C., 2013. An Interpretation of the Origins of the 2012 Central Great Plains Drought Assessment Report.

Hsiang, S.M., Burke, M., Miguel, E., 2013. Quantifying the influence of climate on human conflict. Science 341, 1235367. http://dx.doi.org/10.1126/science.1235367.

IPCC, 2012. Managing the risks of extreme events and disasters to advance climate change adaptation. In: Field, C.B., Barros, V., Stocker, T.F., Dahe, Q. (Eds.), A Special Report of Working Groups I and II of the Intergovernmental Panel on Climate Change. Cambridge University Press, Cambridge. doi: 10.1017/CBO9781139177245.

IPCC, 2013. Annex I: Atlas of global and regional climate projections. In: van Oldenborgh, G.J., Collins, M., Arblaste, J., Christensen, J.H., Marotzke, J., Power, S.B., Rummukainen, M., Zhou, T. (Eds.), Climate Change 2013: The Physical Science Basis. Contribution of Working Group I to the Fifth Assessment Report of the Intergovernmental Panel on Climate Change. Cambridge University Press, Cambridge, United Kingdom and New York, NY, USA, pp. 1311–1394.

Keyantash, J., Dracup, J.A., 2002. The quantification of drought: an evaluation of drought indices. Bull. Am. Meteorol. Soc. 83, 1167–1180. http://dx.doi.org/10.1175/1520-0477.

Kundzewicz, Z., Mata, L., Arnell, N., Döll, P., Jimenez, B., Miller, K., Oki, T., Sen, Z., Shiklomanov, I., 2008. The implications of projected climate change for freshwater resources and their management 53, 3–10. http://dx.doi.org/10.1623/hysj.53.1.3.

Laio, F., 2004. Cramer–von Mises and Anderson-Darling goodness of fit tests for extreme value distributions with unknown parameters. Water Resour. Res. http://dx.doi.org/10.1029/2004WR003204.

Liu, L., Hong, Y., Looper, J., Riley, R., Yong, B., Zhang, Z., Hocker, J., Shafer, M., 2013. Climatological drought analyses and projection using SPI and PDSI : Case study of the Arkansas Red River Basin. J. Hydrol. Eng. 18, 809–816. http://dx.doi.org/10.1061/(ASCE)HE.1943-5584.0000619.

Madadgar, S., Moradkhani, H., 2013. Drought analysis under climate change using copula. J. Hydrol. Eng. 18, 746–759. http://dx.doi.org/10.1061/(ASCE)HE.1943-5584.

McKee, T., Doesken, N., Kleist, J., 1993. The relationship of drought frequency and duration to time scales. Eighth Conf. Appl. Climatol.

Mishra, A.K., Singh, V.P., 2010. A review of drought concepts. J. Hydrol. 391, 202–216. http://dx.doi.org/10.1016/j.jhydrol.2010.07.012.

Mo, K.C., 2008. Model-based drought indices over the United States. J. Hydrometeorol. 9, 1212–1230. http://dx.doi.org/10.1175/2008JHM1002.1.

Myers, N., 2002. Environmental refugees: a growing phenomenon of the 21st century. Philos. Trans. R. Soc. Lond. B Biol. Sci. 357, 609–613. http://dx.doi.org/10.1098/rstb.2001.0953.

Nepstad, D.C., Tohver, I.M., Ray, D., Moutinho, P., Cardinot, G., 2007. Mortality of large trees and lianas following experimental drought in an Amazon forest. Ecology 88, 2259–2269.

Ojha, R., Kumar, D.N., Sharma, A., Mehrotra, R., 2013. Assessing severe drought and wet events over India in a future climate using a nested bias-correction approach. J. Hydrol. Eng. 18, 760–772. http://dx.doi.org/10.1061/(ASCE)HE.1943-5584.0000585.

Oppenheimer, M., Campos, M., Warren, R., Birkmann, J., Luber, G., O'Neill, B., Takahashi, K., 2014. Emergent Risks and Key Vulnerabilities. In: Field, C.B., Barros, V., Mach, K., Mastrandrea, M. (Eds.), Contribution of Working Group II to the IPCC Fifth Assessment Report.

Orlowsky, B., Seneviratne, S.I., 2013. Elusive drought: uncertainty in observed trends and short- and long-term CMIP5 projections. Hydrol. Earth Syst. Sci. 17, 1765–1781. http://dx.doi.org/10.5194/hess-17-1765-2013.

Oubeidillah, A.A., Kao, S.-C., Ashfaq, M., Naz, B.S., Tootle, G., 2014. A large-scale, high-resolution hydrological model parameter data set for climate change impact assessment for the conterminous US. Hydrol. Earth Syst. Sci. 18, 67–84. http://dx.doi.org/10.5194/hess-18-67-2014.

Palmer, M.A., Lettenmaier, D.P., Poff, N.L., Postel, S.L., Richter, B.D., Warner, R., 2009. Climate change and river ecosystems: protection and adaptation options. Environ. Manage. 44, 1053–1068. http://dx.doi.org/10.1007/s00267-009-9329-1.

Phillips, O., Aragão, L., Lewis, S.L., Fisher, J., 2009. Drought sensitivity of the Amazon rainforest. Science (80-.). 323, 1344–1347. http://dx.doi.org/10.1126/science.1164033.

Poff, N.L., Allan, J.D., Bain, M.B., 1997. The natural flow regime. Bioscience 47, 769–784. http://dx.doi.org/10.2307/1313099.

Rao, A.R., Hamed, K., 2000. Flood Frequency Analysis. CRC Press, Boca Raton, FL.

Rind, D., Goldberg, R., Hansen, J., Rosenzweig, C., Ruedy, R., 1990. Potential evapotranspiration and the likelihood of future drought. J. Geophys. Res. Atmos. 95, 9983–10004. http://dx.doi.org/10.1029/JD095iD07p09983.

Rogelj, J., Meinshausen, M., Knutti, R., 2012. Global warming under old and new scenarios using IPCC climate sensitivity range estimates. Nat. Clim. Chang. 2, 248–253. http://dx.doi.org/10.1038/nclimate1385.

Seth, A., Rauscher, S.A., Biasutti, M., Giannini, A., Camargo, S.J., Rojas, M., 2013. CMIP5 projected changes in the annual cycle of precipitation in monsoon regions. J. Clim. 26, 7328–7351. http://dx.doi.org/10.1175/JCLI-D-12-00726.1.

Sheffield, J., Wood, E.F., 2007. Projected changes in drought occurrence under future global warming from multi-model, multi-scenario, IPCC AR4 simulations. Clim. Dyn. 31, 79–105. http://dx.doi.org/10.1007/s00382-007-0340-z.

Shukla, S., Wood, A.W., 2008. Use of a standardized runoff index for characterizing hydrologic drought. Geophys. Res. Lett. 35, 1–7. http://dx.doi.org/10.1029/2007GL032487.

Svoboda, M., LeComte, D., Hayes, M., Heim, R., Gleason, K., Angel, J., Rippey, B., Tinker, R., Palecki, M., Stooksbury, D., Miskus, D., Stephens, S., 2002. The drought monitor. Bull. Am. Meteorol. Soc. 83, 1181–1190.

Taylor, K.E., Stouffer, R.J., Meehl, G.A., 2012. An overview of CMIP5 and the experiment design. Bull. Am. Meteorol. Soc. 93, 485–498. http://dx.doi.org/10.1175/BAMS-D-11-00094.1.

Thornthwaite, C., 1948. An approach toward a rational classification of climate. Geogr. Rev. 38, 55–94.

Trenberth, K.E., Dai, A., Van Der Schrier, G., Jones, P.D., Barichivich, J., Briffa, K.R., Sheffield, J., 2014. Global warming and changes in drought. Nat. Clim. Chang. 4, 17–22. http://dx.doi.org/10.1038/NCLIMATE2067.

Van Huijgevoort, M.H.J., van Lanen, H.A.J., Teuling, A.J., Uijlenhoet, R., 2014. Identification of changes in hydrological drought characteristics from a multi-GCM driven ensemble constrained by observed discharge. J. Hydrol. 512, 421–434. http://dx.doi.org/10.1016/j.jhydrol.2014.02.060.

Vicente-Serrano, S.M., Beguería, S., López-Moreno, J.I., 2010. A multiscalar drought index sensitive to global warming: the standardized precipitation evapotranspiration index. J. Clim. 23, 1696–1718. http://dx.doi.org/10.1175/2009JCLI2909.1.

Wang, L., Chen, W., 2014. A CMIP5 multimodel projection of future temperature, precipitation, and climatological drought in China. Int. J. Climatol. 34, 2059–2078. http://dx.doi.org/10.1002/joc.3822.

Wang, T., Hamann, A., Spittlehouse, D.L., Aitken, S.N., 2006. Development of scale-free climate data for Western Canada for use in resource management. Int. J. Climatol. 26, 383–397. http://dx.doi.org/10.1002/joc.1247.

Wuebbles, D., Meehl, G.A., Hayhoe, K., Karl, T.R., Kunkel, K., Santer, B., Wehner, M., Colle, B., Fischer, E.M., Fu, R., Goodman, A., Janssen, E., Kharin, V., Lee, H., Li, W., Long, L.N., Olsen, S.C., Pan, Z., Seth, A., Sheffield, J., Sun, L., 2013. CMIP5 Climate Model Analyses: Climate Extremes in the United States. Bull. Am. Meteorol. Soc. http://dx.doi.org/10.1175/BAMS-D-12-00172.1.

Zektser, S., Loaiciga, H.A., Wolf, J.T., 2004. Environmental impacts of groundwater overdraft: selected case studies in the southwestern United States. Environ. Geol. 47, 396–404. http://dx.doi.org/10.1007/s00254-004-1164-3.